Angular dependence of the Fermi surface cross-section area and magnetoresistance in quasi-two-dimensional metals

P. D. Grigoriev*
L. D. Landau Institute for Theoretical Physics, Chernogolovka, Russia
(Received 22 February 2010; revised manuscript received 23 April 2010; published 25 May 2010)

The analytical and numerical study of the angular dependence of magnetoresistance in layered quasi-two-dimensional (Q2D) metals is performed. The harmonic expansion analytical formulas for the angular dependence of Fermi-surface cross-section area in external magnetic field are obtained for various typical crystal symmetries. These formulas correct the previous results and allow the simple and effective interpretation of the magnetic quantum oscillations data in cuprate high-temperature superconducting materials, in organic metals and in other Q2D metals. Another analytical result for the azimuth-angle dependence of the Yamaji angles is obtained for the elliptic in-plane Fermi surface. The relation between the angular dependence of magnetoresistance and of Fermi-surface cross-section area is derived. The applicability region of all results obtained is investigated using the numerical calculations.

DOI: 10.1103/PhysRevB.81.205122 PACS number(s): 72.15.Gd, 73.43.Qt, 74.70.Kn, 74.72.−h

I. INTRODUCTION

The layered quasi-two-dimensional (Q2D) compounds attract great attention for their physical properties and promising technical applications. High-temperature cuprate superconductors,[1] organic metals,[2] heterostructures,[3] and intercalated graphites[4] are the examples of these compounds. The knowledge of quasiparticle dispersion in these compounds is very important for understanding their properties and electronic phase diagram. The traditional and powerful tools to determine the Fermi-surface (FS) geometry and the electron dispersion in various metals are the magnetic quantum oscillations (MQO) (Ref. 5) and the angular dependence of magnetoresistance (ADMR).[6] There is a huge amount of publications, devoted to the experimental determination of the FS geometry and electron dispersion in high-temperature cuprate superconductors,[7,8] in MgB_2,[9] in organic metals (see Refs. 6 and 10 for reviews) and in many other Q2D metals. The interpretation of the MQO data is, usually, based on the detailed comparison with the band-structure calculations, which is a complicated and often ambiguous procedure. The interpretation of ADMR is also based on fitting by the numerical calculations with a large number of fitting parameters.[11–13] The quick and effective extraction of the FS geometry and of electron dispersion from the experimental data on MQO and on ADMR requires reliable and simple theoretical formulas.

The general form of the electron dispersion in Q2D compounds with monoclinic or higher crystal symmetry can be expressed as the Fourier series in cylindrical coordinates,

$$\varepsilon(\mathbf{k}) = \sum_{\nu\geq 0,\mu=\text{even}} \epsilon_{\mu\nu}(k)\cos(\nu k_z c^*)\cos(\mu\phi+\phi_{\mu\nu}), \quad (1)$$

where the integers $\nu,\mu\geq 0$, the electron momentum $\mathbf{k}=(k_x,k_y,k_z)$ (we set $\hbar=1$), c^* is the interlayer lattice constant, $k=\sqrt{k_x^2+k_y^2}$ is the absolute value of the in-plane momentum, and $\phi=\arctan(k_y/k_x)$ is the azimuth angle of electron momentum. In triclinic crystals the only symmetry constraint on the electron dispersion is $\varepsilon(\mathbf{k})=\varepsilon(-\mathbf{k})$, and the electron dispersion (1) may also contain the additional terms

$$\Delta\varepsilon(\mathbf{k}) = \sum_{\nu>0}\sum_{\mu=\text{odd}} \epsilon_{\mu\nu}(k)\sin(\nu k_z c^*)\cos(\mu\phi+\phi_{\mu\nu}). \quad (2)$$

For simplicity, below we only consider the case of monoclinic or higher crystal symmetry, where the terms (2) are absent.

Usually, it is sufficient to keep only the first few terms in the infinite series (1). If the interlayer transfer integral of conducting electrons $t_c(\phi)\sim\epsilon_{01}$ is much smaller than the in-plane Fermi energy ϵ_{00}, the tight-binding approximation can be used, and one keeps only the terms with $\nu=0$ and $\nu=1$,

$$\varepsilon(\mathbf{k}) = \varepsilon(k,\phi) - 2t_c(\phi)\cos(k_z c^*). \quad (3)$$

The FS, being given by the equation $\varepsilon(\mathbf{k})=E_F$, is a warped cylinder in Q2D compounds. If magnetic field is applied along the z axis of the Q2D metals with the electron dispersion (3), there are two extremal FS cross-section areas A_{ext} encircled by the closed curves $\varepsilon(k_x,k_y)\pm 2t_c=E_F$. Hence, the two close fundamental frequencies $F_{1,2}=(c/2\pi e\hbar)A_{\text{ext}}$ appear in MQO, giving the beats of MQO.[5] The temperature dependence of the MQO amplitude gives the cyclotron mass for the extremal orbit: $m^*_{\text{ext}}\equiv(1/2\pi)[\partial A_{\text{ext}}/\partial E]$. The beat frequency $\Delta F=F_1-F_2$ gives the interlayer transfer integral: $4t_c=\Delta F(e\hbar/m^*_{\text{ext}}c)$. The difference of the two extremal cross-section areas $\Delta A_{\text{ext}}=2\pi e\hbar\Delta F/c$ and, hence, the beat frequency depend on the magnetic field direction, which we denote by the tilt angle θ of magnetic field $\mathbf{B}$ with respect to the z axis (the polar angle) and by the azimuth angle φ of the rotation around the z axis: $\tan\varphi=B_y/B_x$ (see Fig. 1). We use the symbol ϕ for the azimuth angle of electron momentum, and the symbol φ for the azimuth angle of $\mathbf{B}$.

For the axially symmetric FS of the warped-cylinder shape, ΔA_{ext} does not depend on the azimuth angle φ and has rather simple angular dependence[14]

$$\Delta A_{\text{ext}} \propto J_0(c^* k_F \tan\theta), \quad (4)$$

where J_0 is the Bessel function and k_F is the in-plane Fermi momentum. Equation (4) is valid in the first order in the interlayer transfer integral t_c and was first derived geometrically by Yamaji[14] to explain the angular magnetoresistance

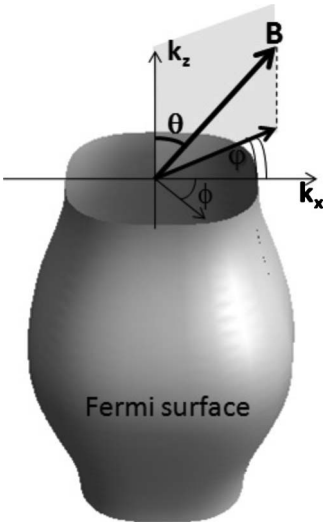

FIG. 1. The illustration of the FS shape, given by Eq. (32), with the explanation of the angle notations, used in the text. The parameters $m=4$, $\beta=0.05$ and $2C_1t_c/E_F=0.2$.

oscillations (AMRO)[15] in Q2D organic metals. Since the difference between the two extremal cross-section areas is proportional to the interlayer transfer integral $t_c(\theta)$, Eq. (4) suggests that the interlayer transfer integral has the similar angular dependence

$$t_c(\theta) \approx t_c(0)J_0(c^*k_F \tan\theta), \tag{5}$$

which gives a strong angular dependence of interlayer conductivity $\sigma_{zz} \propto t_c^2(\theta)$. Equation (5) was later confirmed by the quantum-mechanical calculation of the amplitude of interlayer electron tunneling in tilted magnetic field.[16] The angles θ_m, for which the Bessel function has zeros,

$$J_0(c^*k_F \tan\theta_m) = 0, \tag{6}$$

are called the Yamaji angles and used to determine the in-plane Fermi momentum k_F. At these angles both the interlayer magnetoresistance and the amplitude of MQO have maxima. Usually, the in-plane electron dispersion $\varepsilon(k_x,k_y)$ is anisotropic, and Eqs. (4)–(6) acquire a φ-dependent correction. There is a considerable practical need of the simple analytical formula for the φ dependence of AMRO and MQO, which can be used to extract the in-plane electron dispersion from the experimental data.

The widely used analytical result for the φ dependence of the FS cross section, derived by Bergemann *et al.*[8] and given by Eq. (24) below, takes the FS corrugation only in the first order, which is not enough to obtain correctly even the main φ-dependent term in the angular dependence of the cross-section area. Another simple and widely used[17–20] analytical result for the φ dependence of AMRO maxima (Yamaji angles),

$$\tan\theta_n \approx \pi(n-1/4)/p_B^{\max}c^*, \tag{7}$$

with $p_B^{\max}=p_B^{\max}(\varphi)$ being the maximum value of the Fermi momentum projection on the in-plane magnetic field direction, was derived[17] from the Shockley tube integral[21] using the saddle point approximation. This approximation assumes that the z component of the electron velocity oscillates rapidly when the electron moves along its closed classical orbit in the momentum space in magnetic field. This is valid only at high tilt angles θ of magnetic field, when $\tan\theta \gg 1/c^*p_B^{\max}(\varphi)$, and only in the very clean samples with $\omega_c\tau\cos\theta \gg 1$, where ω_c is the cyclotron frequency and τ is the electron mean free time. For small tilt angle θ this derivation is not applicable, because even for the first Yamaji angle $c^*p_B^{\max}(\varphi)\tan\theta \approx 1$. Below we show that Eq. (7) is valid only for the elliptical FS in the limit $\omega_c\tau\cos\theta \gg 1$. With some small error it can also be applied to the FS, which is close to elliptical. However, Eq. (7) gives completely wrong result for the φ dependence of Yamaji angles when the in-plane FS has tetragonal (as in cuprate high-T_c superconductors) or hexagonal [as in MgB_2 (Ref. 9) or intercalated graphites[4]] symmetry.

The aim of the present paper is to derive the new suitable analytical formulas for the φ dependence of the FS cross-section area, Yamaji angles, and magnetoresistance, which can be used to extract the FS parameters from the experimental data. The applicability region of some previous and widely used results will also be studied.

In Sec. II, we derive the exact expression for the Yamaji zeros for the elliptical FS shape. The deviations from this result for nonelliptic FS is also studied. In Sec. III, we find the main φ-dependent correction to the FS cross-section area for the anisotropic dispersion $\varepsilon(k_x,k_y)$ in Eq. (3), when the in-plane anisotropy of the FS is weak. As will be shown, this result has wide applicability region and can also be applied to almost square-shaped in-plane FS as in the high-T_c cuprate superconductors. In Sec. IV, we discuss how the obtained results can help to observe and to analyze the MQO. In particular, we discuss the optimal field directions to observe the φ dependence of MQO frequency. In Sec. V, we derive and specify the applicability region of the relation between the k_z dependence of the FS cross-section area and the angular dependence of background magnetoresistance. This relation shows, that the geometrical and resistivity Yamaji angles coincide in the limit $\omega_c\tau\cos\theta \gg 1$ and $t_c/E_F \ll 1$. The discussion and the summary of the results is given in Sec. VI.

II. ELLIPTIC FERMI SURFACE

First, we derive the analytical formula for the Yamaji angles for the elliptic in-plane dispersion

$$\varepsilon(k_x,k_y) \equiv k_x^2/2m_x + k_y^2/2m_y = \varepsilon(k)[1+\beta\cos 2\phi], \tag{8}$$

where $\varepsilon(k)=k^2/2m$, $m \equiv 2m_xm_y/(m_x+m_y)$, and $\beta \equiv (m_x-m_y)/(m_x+m_y)$. The shape of the FS for this dispersion is, of cause, also elliptical. The ellipse can be obtained from the circle by the dilation Λ_x along one in-plane direction (along the x axis): $x \to \lambda x$. Consider the cross-section area of the FS by the plane, cutting the k_z axis at the point k_{z0}, and perpendicular to the magnetic field direction $\mathbf{B}=B\mathbf{n}$, where the unit vector

$$\mathbf{n} = (n_x,n_y,n_z) = (\sin\theta\cos\varphi, \sin\theta\sin\varphi, \cos\theta). \tag{9}$$

For the circular in-plane FS this cross-section area is independent of the angle φ. In the first order in t_c/E_F, it is also

independent of k_{z0} at special directions $\mathbf{n}_{\mathrm{Yam}}$, corresponding to the Yamaji angles $\theta=\theta_{\mathrm{Yam}}$, given by Eq. (6). After the dilation Λ_x, the direction of magnetic field, which is perpendicular to the cross-section plane, also changes,

$$\mathbf{n} \to \Lambda_x(\mathbf{n}) = \frac{(n_x/\lambda, n_y, n_z)}{\sqrt{(n_x/\lambda)^2 + n_y^2 + n_z^2}}. \tag{10}$$

However, the cross-section area perpendicular to $\mathbf{n}_1 = \Lambda_x(\mathbf{n}_{\mathrm{Yam}})$ remains independent of k_{z0} if it was independent before the dilation. Hence, the direction $\mathbf{n}_1=\Lambda_x(\mathbf{n}_{\mathrm{Yam}})$ corresponds to the new Yamaji angle $\theta_{\mathrm{Yam}}(\varphi)$. The polar and azimuthal angles are related to the components of the vector $\mathbf{n}_1=(n_{1x}, n_{1y}, n_{1z})$ as

$$\tan\,\theta_1 = \frac{\sqrt{n_{1x}^2 + n_{1y}^2}}{n_{1z}}, \quad \tan\,\varphi_1 = \frac{n_{1y}}{n_{1x}}. \tag{11}$$

Combining above equations we obtain the relation between the old and new Yamaji angle $\theta^*_{\mathrm{Yam}}=\Lambda_x(\theta_{\mathrm{Yam}})$

$$\frac{\tan\,\theta^*_{\mathrm{Yam}}}{\tan\,\theta_{\mathrm{Yam}}} = \frac{\sqrt{n_x^2/\lambda^2 + n_y^2}}{n_z \tan\,\theta_{\mathrm{Yam}}} = \sqrt{\frac{\cos^2\,\varphi}{\lambda^2} + \sin^2\,\varphi}.$$

The angle φ here is the angle before the dilation Λ_x. It is related to the angle φ_1 after the dilation as

$$\tan\,\varphi_1 = \lambda\,\tan\,\varphi.$$

Then, after simple trigonometric algebra, we obtain

$$\begin{aligned}\frac{\tan\,\theta^*_{\mathrm{Yam}}}{\tan\,\theta_{\mathrm{Yam}}} &= \frac{\cos\,\varphi}{\lambda}\sqrt{1+\tan^2\,\varphi_1} \\ &= \frac{\sqrt{1+\tan^2\,\varphi_1}}{\sqrt{\lambda^2+\tan^2\,\varphi_1}} \\ &= \frac{1}{\sqrt{\lambda^2\,\cos^2\,\varphi_1 + \sin^2\,\varphi_1}}.\end{aligned} \tag{12}$$

For the elliptic dispersion (8) the maximum value of the Fermi momentum projection on the in-plane magnetic field direction is given by

$$p_B^{\max} = \sqrt{(p_1\,\cos\,\varphi)^2 + (p_2\,\sin\,\varphi)^2}, \tag{13}$$

where $p_1^2=2m_x\varepsilon_F$ and $p_2^2=2m_y\varepsilon_F$. The r.h.s. of Eq. (12) coincides with $p_2/p_B^{\max}$. Hence, the generalization of the Yamaji zeros to the elliptic dispersion (8) writes down as

$$J_0[c^* p_B^{\max}(\varphi)\tan\,\theta_n] = 0. \tag{14}$$

Approximately, Eq. (14) coincides with Eq. (7), derived for the interlayer conductivity[6,17] from the Shockley tube integral.[21] The saddle point approximation, used in Ref. 17 to derive Eq. (7), assumes that the z component of electron velocity oscillates rapidly when the electron moves along its closed orbit in the momentum space. This is valid only at high-tilt angles θ of magnetic field, when $\tan\,\theta \gg 1/c^* p_B^{\max}(\varphi)$, and only in very clean samples with $\omega_c\tau\,\cos\,\theta \gg 1$. These two conditions are very rarely satisfied together. The reason, why Eq. (7) describes well some experimental data,[6] comes from its coincidence with the exact geometrical expression (14) for the Yamaji angles for the elliptic Fermi surface, which according to Eq. (48) gives the maxima of magnetoresistance. With some small error, Eqs. (14) and (7) can be applied to any elongated FS (see Fig. 2). However, for the FS with tetragonal or hexagonal in-plane symmetry, Eqs. (14) and (7) give completely incorrect result (see Fig. 3). Hence, another approach is need for such FS geometry, which is proposed in the next section.

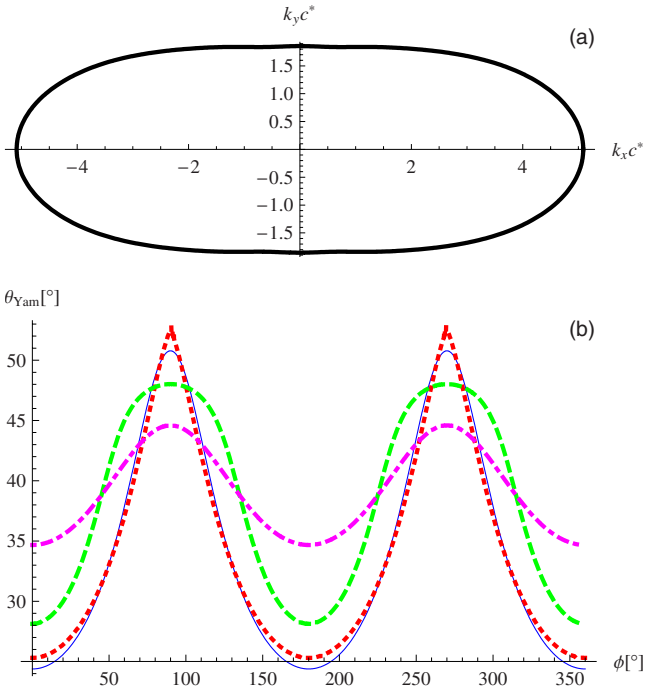

FIG. 2. (Color online) The in-plane FS shape (a) and the first Yamaji angle as function of the azimuth angle φ (b) for the elongated FS with monoclinic symmetry and the Fermi momentum given by $k_0(\phi)=\Sigma_{j=0}^4 k_{4j0}\,\cos(4j\phi)$ with $\beta=k_{40}/k_{00}=0.5$. The higher harmonics are added to smooth the FS [see (a)]. The blue solid curve [see (b)] is the numerical result for the first Yamaji angle, obtained using Eq. (27); the red dotted curve is the result of Eq. (14); the green dashed curve is the result from Eq. (34) and magenta dash-dotted curve is the result from Eq. (24) and used in Refs. 8 and 22. One can see that Eq. (14) gives the best result for Yamaji angles when the FS is strongly elongated. The harmonic expansion still gives a reasonable result, though the coefficient $\beta=0.5\sim1$ is not small. The result of Eq. (24) gives much weaker φ-dependence than the correct one.

III. HARMONIC EXPANSION OF THE CROSS-SECTION AREA

The dependence of the Fermi momentum $k_F(\phi,k_z)$ on the azimuthal angle ϕ and the momentum component k_z can be expanded in the Fourier series,[8]

$$k_F(\phi,k_z) = \sum_{\nu\geq 0} k_\nu(\phi)\cos(\nu k_z c^*), \tag{15}$$

$$= \sum_{\mu,\nu\geq 0} k_{\mu\nu}\,\cos(\nu k_z c^*)\cos(\mu\phi + \phi_{\mu\nu}). \tag{16}$$

The relation between the first coefficients in the expansions (16) and (1) is given in Appendix. The influence of various

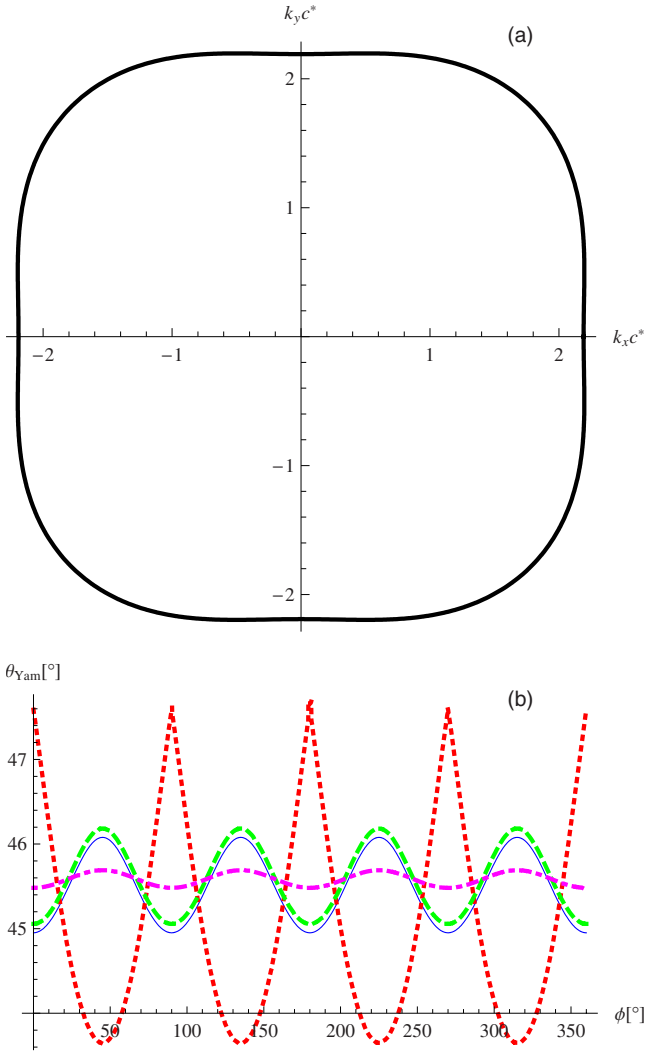

FIG. 3. (Color online) The in-plane FS shape (a) and the first Yamaji angle as function of the polar angle ϕ (b) for the FS with tetragonal symmetry and the Fermi momentum given by Eq. (32) with $\beta=-0.07$. (a) shows that even for very small parameter β the in-plane FS strongly differs from the circle. It is almost quadratic. Hence, the harmonic expansion of the ϕ dependence of the FS shape is applicable for most compounds with tetragonal symmetry. In (b) the blue solid curve is the numerical result for the first Yamaji angle, obtained using Eq. (27). The red dashed curve is the result of Eq. (14); it gives too strong and opposite ϕ dependence, which is completely incorrect. The green dotted curve is the result from Eq. (34); it gives very good agreement with the numerical result. The magenta dash-dotted curve illustrates Eq. (24), used by Bergemann *et al.* (Refs. 8 and 22); this result gives too weak ϕ dependence in agreement with the discussion in the end of Secs. III A and VI.

harmonics $k_{\mu\nu}$ on the FS shape is illustrated in the Table I in Ref. 8 and in Table 4 of Ref. 22. The phase $\phi_{\mu\nu}$ in Eq. (16) is, usually, zero, but it can also be $\pi/2$ for odd ν and special crystal symmetry (see Sec. III B).

Consider arbitrary direction of magnetic field **B**, given by the polar and azimuthal angles θ and φ, and the plane perpendicular to this field in the momentum space, which cuts the k_z axis at $k_z=k_{z0}$. The Fermi surface cross-sectional area $A=A(k_{z0},\theta,\varphi)$ by this pane is given by the integral

$$A(k_{z0},\theta,\varphi)=\int_0^{2\pi} d\phi' k_F^2(\varphi+\phi',k_z)/(2\cos\theta), \quad (17)$$

where integration variable ϕ' is the difference between azimuth angles of a point on the FS and of the magnetic field direction, and k_z at this FS point satisfies the equation

$$k_z=k_{z0}-k_F(\varphi+\phi',k_z)\tan\theta\cos\phi'. \quad (18)$$

Equations (17) and (18) allow us to calculate the cross-section area $A(k_{z0},\theta,\varphi,k_F c^*)$ numerically for any given FS, determined by the function $k_F(\phi,k_z)$ or, equivalently, by the coefficients $k_{\mu\nu}$ in expansion (16). In practice, one usually solves the inverse problem of the extraction of FS parameters from the experimental data on MQO or AMRO. Then, the direct procedure of fitting the experimental data by the parameters $k_{\mu\nu}$ in expansion (16) is rather ambiguous because of too large number of fitting parameters. Usually, the coefficients $k_{\mu\nu}$ fall down rapidly with increasing μ and ν. Therefore, it is useful to fit only the first few terms in the similar harmonic expansion of the cross-section area

$$A(k_{z0},\theta,\varphi)=\sum_{\mu,\nu} A_{\mu\nu}(\theta)\cos[\mu\varphi+\delta_{\mu\nu}]\cos(\nu c^* k_{z0}), \quad (19)$$

keeping only the first few terms in expansion (16). The first coefficients $A_{\mu\nu}(\theta)$ can be found analytically in the main order in $k_{\mu\nu}$. The analytical formula for the coefficients $A_{\mu\nu}(\theta)$ of the cross-section area is especially useful because of their rather complicated dependence on θ. In Sec. IV, it will be shown that the coefficient $A_{\mu 1}(\theta)$ is directly related to the angular dependence of magnetoresistance at $\omega_c\tau\gg 1$ and $t_c/E_F\ll 1$.

In the zeroth order in coefficients $k_{\mu\nu}$ in expansion (16), i.e., for cylindrical FS neglecting any warping and x-y asymmetry, one obtains the trivial result $A^{(0)}=\pi k_F^2/\cos\theta$, where $k_F\equiv k_{00}$. In the first order in these coefficients $k_{\mu\nu}$, one can neglect the dependence $k_F(\phi,k_z)$ in Eq. (18) and substitute

$$k_z\approx k_{z0}-k_F\tan\theta\cos\phi' \quad (20)$$

to Eqs. (16) and (17). This gives the first-order correction to the cross-section area,

$$A^{(1)}(k_{z0},\theta,\varphi)=\int_0^{2\pi} d\phi' \frac{k_F^2(\varphi,\phi',k_{z0})-k_{00}^2}{2\cos\theta}$$
$$\approx \int_0^{2\pi}\frac{k_{00}d\phi'}{\cos\theta}\sum_{\mu,\nu\geq 0}{}' k_{\mu\nu}\cos[\mu(\varphi+\phi')+\phi_\mu]$$
$$\times\cos[\nu(k_{z0}-k_F\tan\theta\cos\phi')c^*], \quad (21)$$

where the sum $\Sigma'_{\mu,\nu\geq 0}$ does not contain the term $\mu=\nu=0$. Since μ is even, one can replace in the integrand (here and later we introduce the notation $\kappa\equiv k_F c^*\tan\theta$)

$$\cos[\nu(k_{z0}-k_F\tan\theta\cos\phi')c^*]$$
$$\to\cos[\nu k_{z0}c^*]\cos[\nu\kappa\cos\phi']. \quad (22)$$

One can also replace in the integrand

$$\cos[\mu(\varphi+\phi')+\phi_\mu]\to\cos[\mu\varphi+\phi_\mu]\cos[\mu\phi'], \quad (23)$$

because all odd terms vanish after the integration over ϕ'. Then, after the integration over ϕ', the correction $A^{(1)}$ in the first order in $k_{\mu\nu}$ writes down as

$$A^{(1)}=\frac{2\pi k_{00}}{\cos\theta}\sum_{\mu,\nu\geq 0}{}'(-1)^{\mu/2}k_{\mu\nu}\times\cos[\mu\varphi+\phi_{\mu\nu}]\cos(\nu k_{z0}c^*)J_\mu(\nu\kappa) \quad (24)$$

in agreement with Eq. (2) of Ref. 8. Since the Bessel function $J_\mu(0)=0$ for $\mu\neq 0$, all terms $\sim k_{\mu 0}$ vanish in Eq. (24). This is natural, because in the zeroth order in t_c the cross-section area

$$A^{(0)}(k_{z0},\theta,\varphi)=\int_0^{2\pi}d\phi'\frac{k_0^2(\varphi+\phi')}{2\cos\theta} \quad (25)$$

is independent of φ. Hence, to extract any information about the ϕ dependence of the FS, one needs to consider the first order in t_c/E_F, i.e., to find $A_{\mu 1}(\theta)$. Thus, the φ dependence of the cross-section area starts from the term $k_{\mu 1}$, which is of the same order as the second order term $k_{\mu 0}k_{01}/k_F$ [see Eq. (A9)]. Since Eq. (24) or Eq. (2) in Ref. 8, is derived only in the first order in $k_{\mu\nu}$ [see Eqs. (20) and (21)], the result Eq. (24) does not give the correct φ dependence of the cross-section area even in the lowest φ-dependent order. This is illustrated below in Figs. 2 and 3. The extraction of the higher harmonics using Eq. (24) is even more incorrect.

Let us calculate more accurately the lowest-order φ-dependent term in the cross-section area, which is given by the coefficient $A_{\mu 1}(\theta)$ in the Fourier expansion (19). At $t_c\ll E_F$, it is sufficient to take the FS shape in the first order in t_c, given by Eq. (A4). Then, with the same accuracy, Eq. (17) rewrites

$$A(k_{z0},\theta,\varphi)\approx\int_0^{2\pi}d\phi'\frac{k_0^2(\varphi+\phi')}{2\cos\theta}\times\left[1+\frac{2k_1(\varphi+\phi')}{k_0(\varphi+\phi')}\cos(k_zc^*)\right]. \quad (26)$$

Substituting Eqs. (18) and (22), we obtain the following expression for the k_z-dependent correction to $A(k_{z0},\theta,\varphi)$:

$$A_1=\frac{\cos[c^*k_{z0}]}{\cos\theta}\int_0^{2\pi}d\phi'k_0(\phi')k_1(\phi')\times\cos[c^*k_0(\phi')\tan\theta\cos(\phi'-\varphi)]. \quad (27)$$

Here, we also changed the integration variable: $\phi'\to\phi'+\varphi$. The Yamaji formula (4) is easily obtained from Eq. (27) after taking $k_0(\phi)=k_F=\text{const}$ and $k_1(\phi)=C_1(2t_c/E_F)k_F=\text{const}$ and the integration over ϕ', which gives

$$A_{01}(\theta)=\frac{2t_c}{E_F}C_1\frac{2\pi k_F^2}{\cos\theta}J_0(\kappa), \quad (28)$$

where the dispersion-dependent constant

$$C_1\equiv(E_F/k_F)/(\partial\varepsilon_{00}/\partial k)|_{k=k_F}\sim 1. \quad (29)$$

The lowest-order φ dependence of the cross-section area is determined by the Fourier coefficient $A_{m1}(\theta)$, given by

$$A_{m1}(\theta)=\int_0^{2\pi}\frac{\cos(m\varphi+\phi_{m1})d\varphi}{\pi\cos\theta}\frac{A_1(k_{z0},\theta,\varphi)}{\cos[c^*k_{z0}]}. \quad (30)$$

Performing the integration over φ, we obtain

$$A_{m1}(\theta)=\frac{2(-1)^{m/2}}{\cos\theta}\int_0^{2\pi}d\phi'k_0(\phi')k_1(\phi')\times\cos(m\phi'+\phi_{m1})J_m[c^*k_0(\phi')\tan\theta]. \quad (31)$$

To go further, we need to specify the functions $k_0(\phi)$ and $k_1(\phi)$. We distinguish two symmetries of electron dispersion, namely, with straight and ϕ-dependent (corrugated in the main order) interlayer transfer integral.

A. Straight interlayer hopping

When the in-plane FS anisotropy is weak, one can keep only the first ϕ-dependent terms in the Fourier expansion of the functions $k_0(\phi)$ and $k_1(\phi)$. If the crystal symmetry allows the ϕ-independent (straight) interlayer coupling, these functions expand as

$$k_0(\phi)\approx(1+\beta\cos m\phi)k_F,$$

$$k_1(\phi)\approx\frac{2t_cC_1}{E_F}(1+\beta_1\cos m\phi)k_F, \quad (32)$$

where m is an even integer number, $|\beta|,|\beta_1|\ll 1$ and the constant $C_1\sim 1$ is given by Eq. (29): $2t_cC_1/E_F=k_{01}/k_{00}$. The corresponding FS shape is illustrated in Fig. 1. This type of symmetry is the most common. For example, the electron dispersion adopted to describe the high-T_c superconductors YBCO, Bi2212, Tl2212, and containing the interlayer transfer integral of the form[23] $t_\perp(\mathbf{k})=(t_\perp/4)[\cos(k_xa)-\cos(k_ya)]^2$, gives the FS of the form (32) with $m=4$ and $\beta_1=1$, where all higher harmonics are negligible.

Now we expand the Bessel function $J_m[c^*k_0(\phi')\tan\theta]$ in Eq. (31) in the small parameter $\beta\kappa$ up to the first order (for the first Yamaji angle $\kappa\equiv c^*k_F\tan\theta\approx 2.4\sim 1$). Then the integral over ϕ' in Eq. (31) simplifies to

$$\int_0^{2\pi}d\phi'(\beta+\beta_1)\cos(m\phi')\cos(m\phi')J_m(\kappa)+\int_0^{2\pi}d\phi'\cos(m\phi')J_m'(\kappa)\kappa\beta\cos(m\phi')=\pi\beta\{J_m(\kappa)(1+\beta_1/\beta)+J_m'(\kappa)\kappa\},$$

where the derivative

$$J_m'(\kappa)=\frac{dJ_m(\kappa)}{d\kappa}=\frac{m}{\kappa}J_m(\kappa)-J_{m+1}(\kappa).$$

Hence, in the first order in β,β_1 we obtain

$$A_{m1}(\theta) = (-1)^{m/2} \frac{4\pi k_F^2 C_1 \beta t_c}{E_F \cos\theta} \times \left[J_m(\kappa)\left(1 + \frac{\beta_1}{\beta} + m\right) - \kappa J_{m+1}(\kappa) \right]. \quad (33)$$

Combining the results Eqs. (19), (28), and (33), we obtain the cross-section area

$$A(k_{z0}, \theta, \varphi) \approx \frac{\pi k_F^2}{\cos\theta} + \frac{4\pi k_F^2 t_c C_1}{E_F \cos\theta} \cos[c^* k_{z0}] \times \{J_0(\kappa) + \beta(-1)^{m/2}[(1 + \beta_1/\beta + m)J_m(\kappa) - \kappa J_{m+1}(\kappa)]\cos(m\varphi)\}. \quad (34)$$

The ratio β_1/β, entering this formula, can also be expressed via the FS parameterization, given by Eq. (16): $\beta \equiv k_{\mu 0}/k_{00}$, $\beta_1 = k_{\mu 1}/k_{01}$, $\beta_1/\beta = k_{\mu 1}k_{00}/k_{01}k_{\mu 0}$. The constant $C_1 = E_F k_{01}/2t_c k_{00}$ relates the value of t_c and the geometrical FS corrugation. It does not influence the Yamaji angles. However, it changes the beat frequency of the magnetic quantum oscillations and the amplitude of the φ-dependent term in the cross-section area. For the typical dispersion of the form (A6), when the relation Eq. (A7) satisfies, the ratio $\beta_1/\beta = 1$ and the constant $C_1 = 1$. For arbitrary dispersion, $\beta_1/\beta \sim 1$ and $C_1 \sim 1$.

The difference between two analytical results, given by Eqs. (34) and (24), is very strong: the factor $J_m(\kappa)$ in Eq. (24) is replaced by the completely different factor $[(1 + \beta_1/\beta + m)J_m(\kappa) - \kappa J_{m+1}(\kappa)]$ in Eq. (34). First, the φ dependence of the cross-section area, predicted by Eq. (34), is stronger approximately by a factor $2+m$ than predicted by Eq. (24) or Ref. 8. Second, it may have different θ-dependence due to the $J_{m+1}(\kappa)$ term, especially for high tilt angles $\kappa \gtrsim 1$. To illustrate the above statement, we plot the results of Eqs. (17), (34), (24), and (14) in Figs. 2 and 3 for the dispersions with monoclinic $m=2$ and tetragonal $m=4$ symmetries.

B. Strongly ϕ-dependent interlayer hopping

In some compounds, e.g. in the high-temperature superconductors Sr_2RuO_4 and $Tl_2Ba_2CuO_{6+\delta}$,[8,11–13] the body-centered tetragonal symmetry of the crystal leads to the ϕ-dependent lowest-order interlayer transfer integral, $t_c(\phi) = t_{c0}\sin(2\phi)$, in the all or some parts of the FS. Then, instead of Eq. (32), we have

$$k_0(\phi) \approx (1 + \beta\cos 2m\phi)k_F,$$

$$k_1(\phi) \approx \frac{2t_c}{E_F} k_F C_1 \sin(m\phi)(1 + \beta_1 \cos 2m\phi). \quad (35)$$

The corresponding FS shape is shown in Fig. 4, where too large value of $t_c = 0.1E_F$ is taken for illustration. Substituting this into Eq. (31) and taking $\beta = \beta_1 = 0$, we obtain the main φ-dependent term, determined by the coefficient

FIG. 4. The illustration of the FS shape given by Eq. (35). The parameters $m=2$, $\beta=0.05$, and $2C_1t_c/E_F=0.2$.

$$A_{m1}(\theta) \approx \frac{2\pi k_F^2 (-1)^{m/2}}{\cos\theta} \frac{2t_c C_1}{E_F} J_m(\kappa) \quad (36)$$

in agreement with the first-order result, given by Eq. (24). This term does not depend on the in-plane FS anisotropy β. To extract this anisotropy in the first order in the φ-dependent interlayer transfer integral, one needs to consider $3m$ harmonic in the cross-section area. For this, we replace in Eq. (31) $m \to 3m$, substitute Eq. (35) and perform the calculation, similar to that in the derivation of Eq. (33). Then, in the lowest order in β, β_1 we obtain

$$A_{3m\ 1}(\theta) = \frac{(-1)^{3m/2}}{\cos\theta} \frac{2\pi t_c C_1}{E_F} \beta k_F^2 \times \left[\left(1 + \frac{\beta_1}{\beta} + 3m\right) J_{3m}(\kappa) - \kappa J_{3m+1}(\kappa) \right]. \quad (37)$$

This result differs from Eq. (33) by the replacement $m \to 3m$ (note that $m=2$ for Sr_2RuO_4 and $Tl_2Ba_2CuO_{6+\delta}$), and the prefactor before the square brackets is two times smaller. The difference between the first-order result of Eq. (24) and the new formula (37) for the $3m$ harmonic is even stronger than in the case of Eq. (33). The total φ-dependence of the cross-section area in the case of φ-dependent interlayer coupling, given by Eq. (35), writes down as

$$A(k_{z0},\theta,\varphi) \approx \frac{\pi k_F^2}{\cos\theta} + \frac{4\pi k_F^2 t_c C_1}{E_F \cos\theta}\cos[c^* k_{z0}] \times \left\{ J_m(\kappa)\sin(m\varphi) + \frac{\beta}{2}(-1)^{3m/2}\left[\left(1+\frac{\beta_1}{\beta}+3m\right)J_{3m}(\kappa) - \kappa J_{3m+1}(\kappa)\right]\sin(3m\varphi)\right\}. \quad (38)$$

This formula can be applied to analyze the experimental data in high-temperature superconductors Sr_2RuO_4, $Tl_2Ba_2CuO_{6+\delta}$, where $m=2$ in Eq. (38), and in some other layered compounds with the appropriate symmetry. Note, that Eqs. (34) and (38) were derived under the condition $\beta\kappa \ll 1$, which is fulfilled in the compounds of tetragonal or hexagonal symmetry at not very high-tilt angle of magnetic field. At very high tilt angle, $\tan\theta > E_F/2t_c$, above derivations are not valid also because of the multiple intersections of the FS by the cross-section plane.

IV. ANALYSIS OF MAGNETIC QUANTUM OSCILLATIONS

The well-resolved magnetic quantum oscillations in Q2D metals give two close frequencies $F_{\max}$ and $F_{\min}$, corresponding to the maximum and minimum of the FS cross-section area. To extract the ϕ dependence of the FS, as follows from Eqs. (34) and (38), one needs to measure the φ dependence of the difference $\Delta F = F_{\max} - F_{\min} \sim 4\pi k_F^2 t_c / E_F$ between these two close frequencies (the beat frequency), which is harder because requires the resolution of MQO in the wider interval of magnetic field. The observation of the beat frequency itself is important because it means the existence of the three-dimensional Fermi surface, i.e., of the coherent interlayer electron transport. Equations (34) and (38) can be used to determine the optimal orientation of magnetic field for the observation of the beat frequency. For straight interlayer electron coupling, given by Eq. (32), the beat frequency has maximum value when magnetic field is perpendicular to the layers, i.e., at polar angle $\theta=0$. However, for the ϕ-dependent interlayer coupling as in Eq. (35), the beat frequency at $\theta=0$ is zero, as follows from Eq. (38). Hence, in this case to observe the beat frequency one needs to incline the magnetic field. The angular dependence of the beat frequency is given by the function in the curly brackets in Eq. (38). The first term $J_m(\kappa)\sin(m\varphi)$ in the curly brackets is much larger than the second. Its maximum gives the optimal orientation $(\theta_{\rm opt}, \varphi_{\rm opt})$ of magnetic field for the observation of MQO beat frequency. For $m=2$, as in Sr_2RuO_4, $Tl_2Ba_2CuO_{6+\delta}$ and some other high-T_c compounds, the factor $J_m(\kappa)\sin(m\varphi)$ has maximum at $\varphi_{\rm opt} = (2n+1)\pi/4$ and $\theta_{\rm opt} \approx \arctan(3.0/k_F c^*)$, where c^* is the interlayer lattice constant. Note, that the spin factor of MQO also depends on the angle θ.[5]

If the beat frequency of MQO cannot be resolved (in dirty materials or at high temperature), the minima of the beat frequency, i.e., the Yamaji angles, can be detected from the increase of the amplitude of MQO. This increase in MQO amplitude happens because at the Yamaji angles the MQO from both extremal electron orbits have the same phase.[5,6] The Yamaji angles can be much easier discerned in the angular dependence of background magnetoresistance (AMRO) (see Sec. V). To determine the φ dependence of the Yamaji angles one can again use Eqs. (34) and (38).

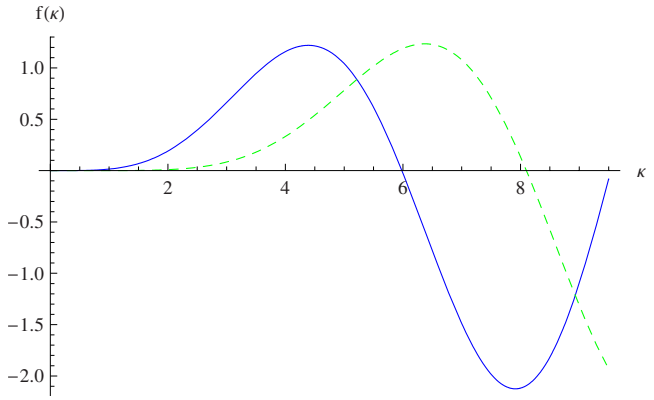

FIG. 5. (Color online) The amplitude of the φ dependence of the extremal cross-section area as function of the polar angle θ for tetragonal (blue solid line) and hexagonal (green dashed line) symmetries in the case of straight interlayer electron hopping.

If the φ dependence of MQO beat frequency is clearly resolved, one can obtain the information about the in-plane FS shape. Eqs. (34) and (38) again can be used to determine the optimal magnetic field orientation for the observation of this φ-dependence. In the case of straight interlayer electron hopping, this φ dependence $\propto\cos m\varphi$ has the maximum amplitude when the factor $f(\kappa) = (1+\beta_1/\beta+m)J_m(\kappa) - \kappa J_{m+1}(\kappa)$ in Eq. (34) has maximum. For typical value $\beta_1/\beta=1$ this factor as function of $\kappa \equiv k_F c^* \tan\theta$ for $m=4$ and $m=6$ is plotted in Fig. 5. The function $f(\kappa)$ has first maximum at $\kappa \approx m$ for $m=4$ and $m=6$ (see Fig. 5). It is reasonable to use only the first maximum, because at high tilt angle of magnetic field the cyclotron mass is large and the amplitude of MQO is too small.

In the case of straight hopping, already the lowest-order harmonic in the φ dependence of the MQO frequency gives the relative amplitude β of the same harmonic in the ϕ dependence of the in-plane Fermi momentum [see Eq. (34)]. In the case of φ-dependent interlayer electron hopping, given by Eq. (35), in the main order, the φ dependence of MQO frequency comes from the ϕ-dependence of the interlayer transfer integral and does not give information about the in-plane FS. To determine the shape of the in-plane FS, one needs to study higher harmonics $\propto\cos(3m\varphi)$ in the MQO frequency. The amplitude of the $\cos(3m\varphi)$ term in MQO frequency is given by the function $f_1(\kappa) = (1+\beta_1/\beta+3m)J_{3m}(\kappa) - \kappa J_{3m+1}(\kappa)$ in Eq. (38) and has first maximum at $\kappa \approx 3m$. This determines the optimal polar angle $\theta_{\rm opt}$, at which this φ dependence is most easily observed. According to Eq. (38), this dependence gives the amplitude of the $2m$ harmonic modulation of the in-plane FS.

V. MAGNETORESISTANCE

To calculate magnetoresistance as a function of the direction (θ,φ) of magnetic field one can use the quasiclassical

Boltzmann transport equation for electrons moving along the closed orbits in magnetic field. This approach gives the Shockley-Chambers formula,[21] which at zero temperature expresses conductivity tensor $\sigma_{\alpha\beta}$ via the integral over the Fermi surface,

$$\sigma_{\alpha\beta}(\theta,\varphi) = \frac{e^2}{4\pi^3\hbar^2}\int dk_{z0}\frac{m_H^*\cos\theta/\omega_H}{1-\exp(-2\pi/\omega_H\tau)} \times \int_0^{2\pi}\int_0^{2\pi} v_\alpha(\psi,k_{z0})v_\beta(\psi-\psi',k_{z0}) \times e^{-\psi'/\omega_H\tau}d\psi' d\psi. \quad (39)$$

Here, the momentum space is parametrized by the momentum component $k_H=k_{z0}\cos\theta$ along the magnetic field by the electron energy E and by the "effective angle" $0<\psi<2\pi$ of the rotation in the cross-section plane. The effective cyclotron mass of the orbit is given by

$$m_H^* \equiv \frac{1}{2\pi}\frac{\partial A}{\partial E} = \frac{1}{2\pi\varepsilon'(k_F)}\frac{\partial A}{\partial k_F}, \quad (40)$$

where $A=A(k_H,E_F)$ is the area of the FS cross-section perpendicular to the magnetic field $\mathbf{B}$ at the momentum $k_H\|\mathbf{B}$. The cyclotron frequency of the orbit $\omega_H\equiv eB/m_H^*c$, and $v_\alpha(\psi,k_H)$ is the component of the electron velocity on the FS. Generally, the mean scattering time τ in the integrand (39) may also depend on the position on the Fermi surface. However, we neglect this dependence because in the simplest theory of spin-independent short-range impurity scattering τ depends only on the density of states at the Fermi level.

For dispersion (3) the electron velocity component along the z axis is a function of k_z only

$$v_z(k_z) = (2c^*t_z/\hbar)\sin(c^*k_z). \quad (41)$$

The k_z coordinate of the FS point K satisfies Eq. (18), where $\varphi+\phi'$ is the azimuthal angle of the projection of the FS point K on the x-y plane. Approximately, this equation can be solved by the iteration procedure. In the zeroth order

$$k_z^{(0)} = k_{z0} - k_F\cos(\phi')\tan\theta, \quad (42)$$

and in the next orders

$$k_z^{(i+1)} = k_{z0} - k_F(\phi'+\varphi,k_z^{(i)})\cos(\phi')\tan\theta. \quad (43)$$

The "angle" ψ entering the Shockley-Chambers formula (39) corresponds to the increment of the cross-section area at a given increment of energy,

$$d\psi = \frac{1}{m_H^*}\frac{dk}{v_\perp} = \frac{dk\,\partial k_\perp}{m_H^*\partial E},$$

where $v_\perp$ is the Fermi velocity in a given point, and $k_\perp$ is the Fermi-momentum component perpendicular to FS. Generally, ψ is different from the angles ϕ' and ϕ of the rotation in the cross section and in the x-y planes. The cross-section area multiplied by $\cos\theta$ is equal to the area of the projection in the x-y plane, and ψ is related to the angle ϕ of the rotation in the x-y plane as

$$\frac{d\psi}{d\phi} = \frac{k_F(\phi,k_z)}{m_H^*\cos\theta}\frac{\partial k_F(\phi,E)}{\partial E}. \quad (44)$$

For cylindrical FS one has $k_F(\phi)=k_F$, and ψ coincides with the angle ϕ.

Now we show that for $\omega_H\tau\gg1$ the minima of $\sigma_{zz}(\theta,\varphi)$, given by Eq. (39), coincide with the minima of the mean-square value of the derivative $(\partial A/\partial k_{z0})$, i.e., with the geometrical Yamaji angles. At $\omega_H\tau\gg1$ the exponent $e^{-\psi'/\omega_H\tau}\approx1$, and Eq. (39) gives

$$\sigma_{\alpha\alpha}(\theta,\varphi) = \frac{e^2}{4\pi^3\hbar^2}\int dk_{z0}\frac{m_H^*\cos\theta/\omega_H}{1-\exp(-2\pi/\omega_H\tau)} \times\left(\int_0^{2\pi} v_\alpha(\psi,k_{z0})d\psi\right)^2. \quad (45)$$

Using Eq. (44) we transform the integral

$$I \equiv \int_0^{2\pi} d\psi v_z(\psi,k_{z0}) = \int_0^{2\pi} d\phi\frac{k_F(\phi,k_z)}{m_H^*\cos\theta}\frac{\partial k_F(\phi,E)}{\partial E}\frac{\partial E}{\partial k_z} = \int_0^{2\pi} d\phi\frac{k_F(\phi,k_z)}{m_H^*\cos\theta}\frac{\partial k_F(\phi,k_z)}{\partial k_z}. \quad (46)$$

The derivative

$$\frac{\partial k_F(\phi,k_z)}{\partial k_z} = \frac{\partial k_F[\phi,k_z(k_{z0},\phi)]}{\partial k_{z0}\cdot(\partial k_z/\partial k_{z0})}. \quad (47)$$

From Eq. (18) in the first order in t_c we obtain $\partial k_z/\partial k_{z0}=1$. Hence, from Eq. (46) we get

$$I = \int_0^{2\pi}\frac{d\phi}{m_H^*\cos\theta}\frac{\partial k_F^2(\phi,k_z)}{2\,\partial k_{z0}} = \frac{\partial A(k_{z0},\theta,\varphi_0)}{\partial k_{z0}m_H^*},$$

where the cross-section area A is given by Eq. (17).

Now from Eq. (45) we get

$$\sigma_{zz}(\theta,\varphi) = \frac{e^2\tau\cos\theta}{8\pi^4\hbar^2}\int\frac{dk_{z0}}{m_H^*}\left[\frac{\partial A(k_{z0},\theta,\varphi)}{\partial k_{z0}}\right]^2. \quad (48)$$

Similar relation without rigorous proof was also proposed in Ref. 17. Equation (48) means that the angular dependence of the interlayer conductivity σ_{zz} and of the mean-squared derivative of the FS cross-section area $\partial A/\partial k_{z0}$ coincide in the limit $\omega_H\tau\gg1$ and $t_c/E_F\ll1$. In particular, the geometrical Yamaji angles coincide with the minima of interlayer conductivity at $\omega_H\tau\gg1$. Fig. 6 illustrates how the angular dependence of conductivity varies with changing $\omega_c\tau$.

VI. DISCUSSION

Above we have obtained the following main results: (i) the exact analytical formula (7) for the Yamaji angles in the case of elliptic Fermi surface (Sec. II); (ii) the analytical formulas (34) and (38) for the main φ-dependent term of the cross-section area $A(k_{z0},\theta,\varphi)$, when the FS corrugation is

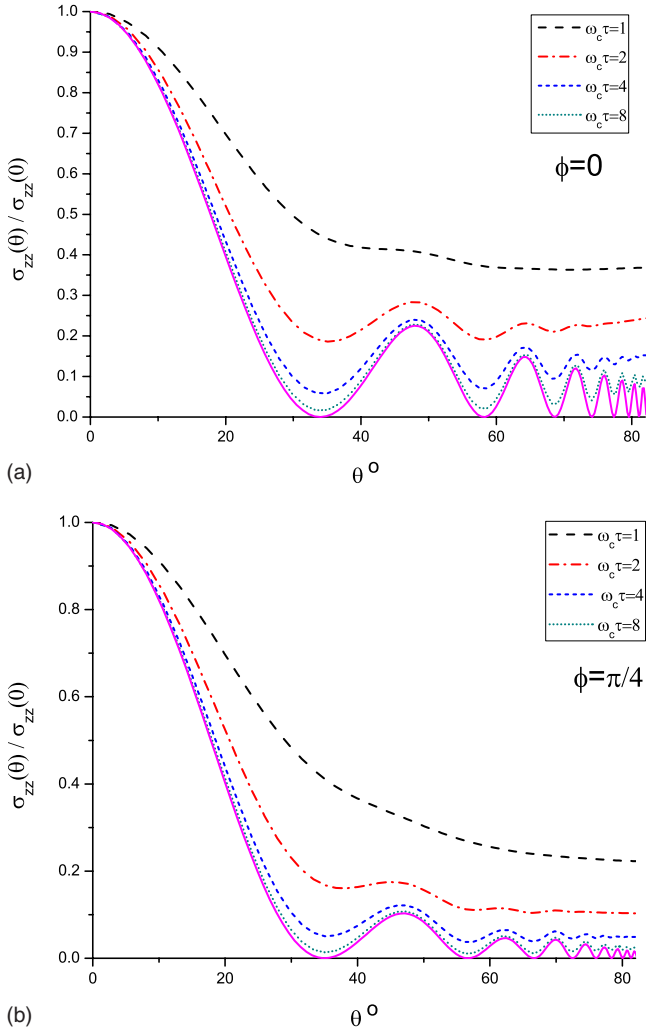

FIG. 6. (Color online) The normalized conductivity σ_{zz}, calculated from Eq. (39) for the dispersion Eq. (49) as function of the polar angle θ for two different azimuthal angles ϕ at several values of $\omega_c\tau=1$ (black dashed line), $\omega_c\tau=2$ (red dash-dotted line), $\omega_c\tau=4$ (blue short-dashed line) and $\omega_c\tau=8$ (green dotted line). The solid magenta line gives the result of Eq. (48).

weak (Sec. III); (iii) the discussion of how these results help to analyze MQO data (Sec. IV); (iv) the derivation and study of a applicability region of Eq. (48), which states, that in the limit $\omega_H\tau \gg 1$ and $t_c/E_F \ll 1$, the angular oscillations of magnetoresistance coincide with the angular oscillations of the k_z-dependent term in the cross-section area. Equation (48) brings additional importance to the results in Secs. II and III for the FS cross-section area. In particular, Eq. (48) means, that the geometrical Yamaji angles $\theta_{\mathrm{Yam}}(\varphi)$ coincide with the maxima of magnetoresistance at $\omega_H\tau \gg 1$.

If the interlayer electron hopping is ϕ dependent, as in Eq. (35), Eq. (48) also suggests the very strong φ dependence of the interlayer magnetoresistance, given by Eq. (38). Note that this φ dependence of magnetoresistance for Sr_2RuO_4 and $Tl_2Ba_2CuO_{6+\delta}$ is in contrast to the so-called "third angular effect," developed in Ref. 24 for the in-plane magnetic field direction. For the Fermi surface in Fig. 3, the third angular effect[24] predicts maxima of conductivity at $\varphi=0$, coinciding with the positions of the FS inflection points, while Eq. (38) predicts these maxima at $\varphi=\pi/4$.

The $\theta-\varphi$ dependence of the cross-section area is an important result because it can be measured from MQO frequency. In Sec IV, we summarized, how formulas (34) and (38) for the cross-section area can be applied to analyze MQO. In particular, these formulas give (i) the optimal direction of magnetic field for the observation of the beats of MQO and of the φ dependence of the beat frequency; (ii) the Yamaji angles, where the magnetoresistance and the amplitude of MQO have maxima; and (iii) the relations between the FS shape and the φ dependence of the beat frequency.

Now we discuss in more details the applicability region of all the above results and compare them with the previous theoretical results. Equations (34) and (38) are derived using the harmonic expansion of the Fermi surface shape, assuming the harmonic amplitudes fall down rapidly with increasing of their number. This turns out to be a very good approximation for any typical FS with the tetragonal or hexagonal symmetry (see Fig. 3) because even a small value of β leads to the strong change in the in-plane FS shape. Thus, for the almost quadratic in-plane FS as in Fig. 3(a), $|\beta|=0.07 \ll 1$. Equations (34) and (38) give bad accuracy only if the in-plane FS is strongly elongated [see Fig. 2(a)]. Fortunately, just for this case Eq. (14) gives the reliable result [see Fig. 2(b)].

Equations (34) and (38) strongly differ from the previous result,[8] given by Eq. (24). The derivation of the result of Bergemann *et al.*[8] does not include the second-order terms in the FS corrugation $k_{\mu\nu}/k_{00}$, which is necessary, because in the first order in $k_{\mu\nu}/k_{00}$, the ϕ dependence of the in-plane FS shape does not enter the φ-dependence of the MQO frequencies. The differences between the old formula of Refs. 8 and 22 and the new formula (34) are illustrated in Figs. 2 and 3 Roughly, the old formula gives too weak φ dependence of the FS cross-section area, which is smaller than the exact result, approximately, by the factor of $2+m$. This leads to the erroneous determination of the FS shape from MQO. In particular, this affects the values of the FS shape parameters of Sr_2RuO_4, extracted from MQO and presented in Table 4 of Ref. 22. Eq. (13) of Ref. 22, used to analyze the MQO data, is the same as the first-order analytical formula given by Eq. (24) above. It allows extracting correctly only those coefficients $k_{\mu\nu}$, which cannot be obtained as the product of much larger coefficients, such as $k_{\mu 0}k_{0\nu}/k_{00}$. Moreover, the coefficient $k_{\mu 0}$ cannot be correctly extracted from Eq. (24) either. In Table 4 of Ref. 22, the reliable extraction using the first-order formula can be performed only for the coefficients k_{00} and k_{21} for the α orbit, the coefficients k_{00} and k_{01} for the β orbit, and the coefficients k_{00} and k_{02} for the γ orbit. All other coefficients in Table 4 of Ref. 22 cannot be accurately extracted using the analytical formulas (13) and (24) of Ref. 22. Equation (24) of Ref. 22 for the angular dependence of the magnetoresistance is also derived in the first order in $k_{\mu\nu}/k_{00}$ and has the same applicability region as Eq. (13) of Ref. 22 or Eq. (24) above. The use of new results, given by Eqs. (34) and (38), allows the accurate extraction of some more coefficients in Table 4 of Ref. 22, for example, the coefficients k_{40} and k_{61} for the α orbit, the coefficients k_{40} and k_{41} for the β orbit, and the coefficients k_{40} and k_{42} for the

γ orbit. However, this extraction is left for the next publications.

The $\theta-\varphi$ dependence of the cross-section area, given by Eqs. (34) and (38), allows us to extract not only the leading in-plane φ dependence of the FS but also to get some information about the Fermi velocity from the coefficient β_1. This would give more information about the electron dispersion. However, the extraction of β_1 is much more difficult than the extraction of β because, according to Eqs. (34) and (38), the dependence of the cross-section area $A_1(\theta,\varphi)$ on β_1 is much weaker than on β. In Figs. 2 and 3, for definiteness, we take the dispersion of form (A6) and $t_c(\phi)$ to be independent on ϕ, which gives Eq. (A9) and $\beta_1/\beta=1$, $C_1=1$ in Eq. (34).

The φ dependence of the Yamaji angles turns out to be weak in the cases of tetragonal or hexagonal symmetry. This dependence is much weaker than the prediction of Eq. (14), used in Refs. 17–20 for the elongated FS, and is much stronger than the prediction of Eq. (24), used in Refs. 8 and 22. For the first Yamaji angle in the case of tetragonal symmetry, Eq. (14) even gives the opposite sign of the φ-dependence of the first Yamaji angle, as can be seeing from Fig. 3(b). For the superelliptic FS, given by Eq. (A8) and discussed in Ref. 18, there is a strong tetragonal modulation of the elliptic FS, and Eq. (14) also fails to give a reliable result.

Equations (34), (38), (14), and (48) are valid only in the first order in the small parameter $t_\perp/\varepsilon_F$. This is, usually, a good approximation for the layered high-T_c superconductors, organic metals, and many other compounds. However, some fine details of the angular dependence of magnetoresistance may be sensitive to the next interlayer hopping term, especially in the case, when the main interlayer hopping is strongly ϕ dependent.

Equations (34), (38), and (14) determine the geometrical Yamaji angles—the conditions for the FS cross section to be almost independent on the interplane momentum k_z, which, according to Eq. (48), gives the minima of conductivity at $\omega_c\tau\to\infty$. To check how strong the conductivity, given by the Shockley-Chambers formula (39), differs from the geometrical formula (48) at finite $\omega_c\tau$, we perform the numerical calculation of the θ dependence of conductivity, $\sigma_{zz}(\theta,\varphi,\omega_c\tau)$, given by Eq. (39), at four different values of $\omega_c\tau=1,2,4,8$ and for two values of the azimuthal angle, $\varphi=0$ and $\varphi=\pi/4$. Then, we compare it with the dependence $\sigma_{zz}(\theta,\varphi)$ given by Eq. (48). The results for the polar-angle dependence of the normalized interlayer conductivity are given in Fig. 6. In this calculation we take the in-plane dispersion, proposed for the layered cuprate high-T_c superconductors and given by

$$\varepsilon(k_x,k_y)=2t_1[\cos(k_xa)+\cos(k_ya)]+4t_2\cos(k_xa)\cos(k_ya)-2t_3[\cos(2k_xa)+\cos(2k_ya)]-E_F, \tag{49}$$

where $a=3.95$ Å is the lattice constant and $t_1=0.38$ eV, $t_2=0.32t_1$, $t_3=0.5t_2$. We take the doping-dependent Fermi energy $E_F=0.02123$ eV. The FS for this dispersion (49) has tetragonal symmetry and is very similar to that in Fig. 3(a) with slightly different values $k_Fa\approx2.14$ at $\varphi=0$ and $k_Fa\approx2.43$ at $\varphi=\pi/4$. Therefore, we do not plot it again. The interlayer hopping term of electron dispersion is taken to be straight (ϕ independent) and given by Eq. (32). From Fig. 6 we see, that the geometrical formula (48) gives rather accurate results for the Yamaji angles of magnetoresistance at $\omega_c\tau\gtrsim2$. For large values of $\omega_c\tau$, the results of Eqs. (48) and (39) coincide. At $\omega_c\tau\lesssim1$ the difference between Eqs. (48) and (39) for the first Yamaji angle reaches 5%–10%. The φ dependence of the Yamaji angles, given by Eqs. (48) and (39), agrees very well; only the amplitude of AMRO reduces with decreasing $\omega_c\tau$.

The background magnetoresistance and, in particular, the saturation values of σ_{zz} at $\theta\to90°$, depend strongly on the azimuthal angle φ (see Fig. 6). Therefore, it is reasonable to use this φ dependence of the conductivity saturation value at $\theta=\pi/2$ to determine the in-plane Fermi surface from the experimental data on the angular dependence of magnetoresistance. The theoretical prediction for this dependence can be obtained from the numerical calculation using the Shockley-Chambers formula (39), as is done in Fig. 6. The origin of this φ dependence is qualitatively explained in Ref. 24.

ACKNOWLEDGMENTS

The work was supported by the Foundation "Dynasty," by RFBR and by MK-2320.2009.2.

APPENDIX: RELATION BETWEEN THE HARMONIC EXPANSIONS OF FERMI MOMENTUM AND OF ELECTRON DISPERSION

The Fermi momentum satisfies the equation

$$\varepsilon[k_F(\phi,k_z),\phi,k_z]=E_F, \tag{A1}$$

where $E_F=\varepsilon(k_F)$ is the Fermi energy. The coefficients $\epsilon_{\mu\nu}$ in Eq. (1) are related to the coefficients $k_{\mu\nu}$ in the FS parametrization (16) through the equation

$$\sum_{\nu\geq0,\mu=\text{even}}\epsilon_{\mu\nu}[k_F(\phi,k_z)]\cos(\nu k_zc^*)\cos(\mu\phi+\phi_{\mu\nu})=E_F. \tag{A2}$$

This equation on $k_{\mu\nu}$ can be solved by the iteration procedure, assuming that the warping coefficients $\epsilon_{\mu\nu}/\epsilon_{00}$ are small and fall down rapidly with increasing μ and ν. In the first order, each term $k_{\mu\nu}$ in the series (16) comes only from the term $\epsilon_{\mu\nu}$ in Eq. (1) with the same indices μ,ν,

$$k_{\mu\nu}^{(1)}=-\epsilon_{\mu\nu}(k_F)/\epsilon_{00}'(k_F). \tag{A3}$$

In the second order in $\epsilon_{\mu\nu}$, the coefficients $k_{\mu\nu}$ come from the interference of the infinite number of the terms $\epsilon_{\mu'\nu'}$ and $\epsilon_{\mu''\nu''}$ in dispersion (1), such that $\mu=\mu'\pm\mu''$ and $\nu=\nu'\pm\nu''$.

For simplicity, we take dispersion (3) and assume that the k_z dependence of the energy is weak, i.e., the interlayer transfer integral $t_c\ll E_F$. The solution of equation

$$\varepsilon(k,\phi)=E_F+2t_c\cos(k_zc^*),$$

in the first order in the interlayer transfer integral $t_c=t_c(\phi)$, gives the FS shape in the cylindrical coordinates,

$$k_F(\phi,k_z) = k_0(\phi) + k_1(\phi)\cos(k_z c^*), \tag{A4}$$

where $k_0(\phi)$ satisfies $\varepsilon[k_0(\phi),\phi]=E_F$ and

$$k_1(\phi) = 2t_c(\phi)/[\partial\varepsilon(k,\phi)/\partial k]|_{k=k_0(\phi)}. \tag{A5}$$

The partial derivative $(\partial\varepsilon/\partial k)|_{k=k_0(\phi)}$ is the projection of the Fermi velocity on the line, connecting the point on the FS with the coordinate origin $\mathbf{k}=0$. It depends on the electron dispersion and on the azimuthal angle ϕ.

For the quite general form of the electron dispersion,

$$\varepsilon(k,\phi) = k^\alpha g(\phi), \tag{A6}$$

where $g(\phi)$ is an arbitrary function and α is also arbitrary, the derivative

$$[\partial\varepsilon(k,\phi)/\partial k]|_{k=k_0(\phi)} = E_F/k_0(\phi). \tag{A7}$$

The superelliptic dispersion

$$\varepsilon(k_x,k_y) = (k_x/k_1)^\alpha + (k_y/k_2)^\alpha, \tag{A8}$$

which includes both linear and quadratic dispersions, is only a particular case of dispersion (A6). With relation (A7), Eq. (A4) simplifies to

$$k_F(\phi,k_z) = k_0(\phi)\left[1 + \frac{2t_c(\phi)}{E_F}\cos(k_z c^*)\right]. \tag{A9}$$

However, relation (A7)) may violate in some compounds, and the application of the simplified formula (A9) instead of Eqs. (A4) and (A5) requires an additional substantiation.

*Present address: Max Planck Institute for the Physics of Complex Systems, Dresden, Germany; grigorev@itp.ac.ru

[1] O. Fischer, M. Kugler, I. Maggio-Aprile, C. Berthod, and C. Renner, Rev. Mod. Phys. **79**, 353 (2007); A. K. Saxena, *High-Temperature Superconductors* (Springer, New York, 2009).

[2] T. Ishiguro, K. Yamaji, and G. Saito, *Organic Superconductors*, 2nd ed. (Springer-Verlag, Berlin, 1998); *The Physics of Organic Superconductors and Conductors*, edited by A. G. Lebed (Springer, New York, 2009.

[3] V. Mitin, V. Kochelap, and M. A. Stroscio, *Quantum Heterostructures: Microelectronics and Optoelectronics* (Cambridge University Press, Cambridge, England, 1999).

[4] M. S. Dresselhaus and G. Dresselhaus, Adv. Phys. **51**, 1 (2002).

[5] D. Shoenberg, *Magnetic Oscillations in Metals* (Cambridge University Press, Cambridge, England, 1984).

[6] M. V. Kartsovnik, Chem. Rev. **104**, 5737 (2004).

[7] B. Vignolle, A. Carrington, R. A. Cooper, M. M. J. French, A. P. Mackenzie, C. Jaudet, D. Vignolles, C. Proust, and N. E. Hussey, Nature (London) **455**, 952 (2008); N. Doiron-Leyraud, C. Proust, D. Le Boeuf, J. Levallois, J.-B. Bonnemaison, R. Liang, D. A. Bonn, W. N. Hardy, and L. Taillefer, *ibid.* **447**, 565 (2007); T. Pereg-Barnea, H. Weber, G. Refael, M. Franz, Nat. Phys. **6**, 44 (2009); A. I. Coldea, J. D. Fletcher, A. Carrington, J. G. Analytis, A. F. Bangura, J. H. Chu, A. S. Erickson, I. R. Fisher, N. E. Hussey, and R. D. McDonald, Phys. Rev. Lett. **101**, 216402 (2008); T. Helm, M. V. Kartsovnik, M. Bartkowiak, N. Bittner, M. Lambacher, A. Erb, J. Wosnitza, and R. Gross, *ibid.* **103**, 157002 (2009).

[8] C. Bergemann, S. R. Julian, A. P. Mackenzie, S. NishiZaki, and Y. Maeno, Phys. Rev. Lett. **84**, 2662 (2000).

[9] A. Carrington, E. A. Yelland, J. D. Fletcher, and J. R. Cooper, Physica C **456**, 92 (2007).

[10] J. Wosnitza, *Fermi Surfaces of Low-Dimensional Organic Metals and Superconductors* (Springer-Verlag, Berlin, 1996); M. V. Kartsovnik and V. N. Laukhin, J. Phys. (France) **6**, 1753 (1996); J. Singleton, Rep. Prog. Phys. **63**, 1111 (2000).

[11] N. E. Hussey, M. Abdel-Jawad, A. Carrington, A. P. Mackenzie, and L. Balicas, Nature (London) **425**, 814 (2003).

[12] M. Abdel-Jawad, J. G. Analytis, L. Balicas, A. Carrington, J. P. H. Charmant, M. M. J. French, and N. E. Hussey, Phys. Rev. Lett. **99**, 107002 (2007).

[13] M. P. Kennett and R. H. McKenzie, Phys. Rev. B **76**, 054515 (2007).

[14] K. Yamaji, J. Phys. Soc. Jpn. **58**, 1520 (1989).

[15] M. V. Kartsovnik, P. A. Kononovich, V. N. Laukhin, and I. F. Schegolev, JETP Lett. **48**, 541 (1988) [Pis'ma Zh. Eksp. Teor. Fiz. **48**, 496 (1988)].

[16] Y. Kurihara, J. Phys. Soc. Jpn. **61**, 975 (1992).

[17] M. V. Kartsovnik, V. N. Laukhin, S. I. Pesotskii, I. F. Schegolev, and V. M. Yakovenko, J. Phys. I **2**, 89 (1992).

[18] M. S. Nam, S. J. Blundell, A. Ardavan, J. A. Symington, and J. Singleton, J. Phys.: Condens. Matter **13**, 2271 (2001).

[19] A. A. House, N. Harrison, S. J. Blundell, I. Deckers, J. Singleton, F. Herlach, W. Hayes, J. A. A. J. Perenboom, M. Kurmoo, and P. Day, Phys. Rev. B **53**, 9127 (1996).

[20] A. F. Bangura, P. A. Goddard, J. Singleton, S. W. Tozer, A. I. Coldea, A. Ardavan, R. D. McDonald, S. J. Blundell, and J. A. Schlueter, Phys. Rev. B **76**, 052510 (2007).

[21] J. M. Ziman, *Principles of the Theory of Solids* (Cambridge University Press, Cambridge, England, 1972).

[22] C. Bergemann, A. P. Mackenzie, S. R. Julian, D. Forsythe, and E. Ohmichi, Adv. Phys. **52**, 639 (2003).

[23] S. Chakravarty, A. Sudbo, P. W. Anderson, and S. Strong, Science **261**, 337 (1993).

[24] A. G. Lebed and N. N. Bagmet, Phys. Rev. B **55**, R8654 (1997)